Available online at www.sciencedirect.com
ScienceDirect
Journal of Electron Spectroscopy and Related Phenomena 162 (2008) 1–7
JOURNAL OF ELECTRON SPECTROSCOPY and Related Phenomena
www.elsevier.com/locate/elspec

Splitting the plasmon peak in high-energy reflection electron energy loss experiments

M. Vos *, M.R. Went

Atomic and Molecular Physics Laboratories, Research School of Physical Sciences and Engineering, The Australian National University, Canberra 0200, Australia

Received 11 April 2007; received in revised form 21 May 2007; accepted 21 May 2007
Available online 25 May 2007

Abstract

Elastic scattering of energetic electrons over large angles (in this study 40 keV and 120°) implies momentum and hence energy transfer from an electron to a nucleus. Due to the large mass of the nucleus (relative to the mass of an electron) this energy transfer is small, but it has recently been shown that it can be resolved in a modern spectrometer. Hence the elastic peak of an overlayer/substrate system splits into different components corresponding to atoms with different mass. Here we extend this type of experiment to the plasmon part of a reflection energy loss spectroscopy (REELS) spectrum. It is shown that, for suitable systems, the plasmon peak of an overlayer/substrate system is split by the same amount as the elastic peak. This is a consequence of the fact that detection of an electron in REELS always requires a large-angle elastic scattering event. Moreover, we show that the relative intensity of the plasmon components contains information on the depth distribution of the scatterers.
© 2007 Elsevier B.V. All rights reserved.

Keywords: Thin films; Elastic electron scattering; Plasmon excitation

1. Introduction

For a long time elastic scattering of electrons from atoms was assumed not to change the kinetic energy of the electron. Recently it has been demonstrated experimentally that for large-angle scattering of energetic electrons this is not strictly true and elastic peaks appear at energy loss values depending on the mass of the scatterer [1,2]. The scattered electron transfers an amount of momentum **q** to a single atom, and this atom acquires (on average) a mean kinetic energy $\overline{E_r}(M) = q^2/2M$ with M the mass of the atom. The energy of the electron is reduced by this recoil energy. Thus, the notion that in elastic collisions the kinetic energy of the electron does not change has to be replaced by the notion that the sum of the kinetic energy of the electron and the scatterer is conserved. Scattering from a compound will result in a number of elastic peaks, each peak corresponding to a scatterer with a certain mass. As the cross sections for elastic scattering are assumed to be well-described by theory, one can use these spectra to obtain information about the composition of the sample [2]. Such an experiment is, in many ways, the electron analogue of Rutherford Backscattering Spectroscopy (RBS) using light ions (usually He^+ ions with MeV energy) and hence the term electron Rutherford Backscattering Spectroscopy (ERBS) was coined to describe these experiments.

We will see later that one difference between ERBS and RBS is that in ERBS Doppler broadening due to the vibrations of the atoms is resolved. If the atom had a momentum **k** *before* the collision, then the recoil energy is given by the difference in kinetic energy of the atom before and after the collision:

$$E_r = \frac{(\mathbf{k}+\mathbf{q})^2}{2M} - \frac{k^2}{2M} = \frac{q^2}{2M} + \frac{\mathbf{q}\cdot\mathbf{k}}{M}. \quad (1)$$

The first term of the final result determines the average recoil energy and the second term describes the Doppler broadening of this peak. Thus, (besides the energy resolution of the experiment) the width of the elastic peak is determined by the momentum distribution of the atoms.

In RBS one uses electronic stopping to determine the depth of the scatterer. The ion creates many electronic excitation on its way in and out of the solid and hence gradually loses its kinetic energy. If the mass of the scatterer is known, then from the measured kinetic energy, one can determine the depth of the scatterer.

* Corresponding author. Tel.: +61 2 6125 4985.
E-mail address: maarten.vos@anu.edu.au (M. Vos).

0368-2048/$ – see front matter © 2007 Elsevier B.V. All rights reserved.
doi:10.1016/j.elspec.2007.05.003

Until now this aspect was missing in ERBS, all information was contained in electrons that did not create electronic excitations at all. Information about the depth distribution can be obtained in ERBS by changing the measurement geometry. For example, by choosing either the incoming or outgoing trajectory more glancing along the surface one obtains spectra with a higher surface sensitivity [3,4]. At first sight this appears all that one can do. Separation of the elastic peaks is of the order of a 1–3 eV, smaller than the energy loss in an electronic excitation (typically of the order of 10 eV). Thus, if an inelastic collision occurs, one generally does not know anymore the kinetic energy lost due to the elastic scattering event. Nearly free-electron materials are an exception,as we will show here.

For nearly free electron metals, for example aluminum, most inelastic scattering events are due to plasmon creation. This excitation has a well-defined energy, which varies slightly with the momentum that the plasmon carries. At zero plasmon momentum the plasmon energy is E_p=15.0 eV, this value increases gradually with the plasmon's momentum [5]. The mean deflection of a 40 keV electron due to plasmon excitation is $\simeq 0.1^\circ$ [6]. Thus, deflection due to plasmon creation will not significantly affect the elastic scattering angle required for the electron to be detected and, as a consequence the experiment measures plasmons with different momenta equally well. In our spectrometer the separation of the elastic peak and the maximum of the plasmon peak was found to be 15.2 eV for Al films.

Experiments measuring the energy loss distribution of electrons scattered from a surface are usually referred to as reflection electron energy loss spectroscopy (REELS) [7]. REELS experiments are usually done at electron energies E_0 of 0.2–5 keV, much lower than the experiment described here (40 keV). At these much higher energies we have to consider the recoil energy $E_r(M)$. The energy at which an electron is detected after deflection from an atom and a plasmon excitation is thus: $E_0 - E_r(M) - E_p$. In this paper we will demonstrate that, for suitable systems the plasmon peak is indeed split into two components depending on the mass of the atom that caused the elastic deflection. Further we will demonstrate that the intensity ratio of these components provides us with information about the depth distribution of the scatterers.

It is important to note that there is an important difference in the way depth resolution is obtained in an an RBS and an ERBS spectrum. In RBS one only needs to know the average energy loss per unit distance traveled. The energy distribution of the electronic excitations created does not matter. In ERBS, using the method described here, retrieval of depth information relies on sharp, well-defined structures in the energy distribution of the created excitations.

2. Experimental details

The experiments were done in the Electron Momentum Spectrometer at the Australian National University. This spectrometer is described extensively elsewhere [8]. We equipped the spectrometer with an additional gun for ERBS measurements (Kimball Physics ELG-2 with a barium oxide cathode for low thermal spread of the beam). The actual geometry for this gun is sketched in Fig. 1. Both analyzer and gun are on a cone with half-angle of approximate 45°. The gun is in the vertical plane through the axis of the cone. The analyzer in the horizontal plane. The corresponding scattering angle is 120°. The peak separation in these 120° scattering experiments [4] is about 5 times larger than the separation in the earlier experiment using a 45° scattering angle [9].

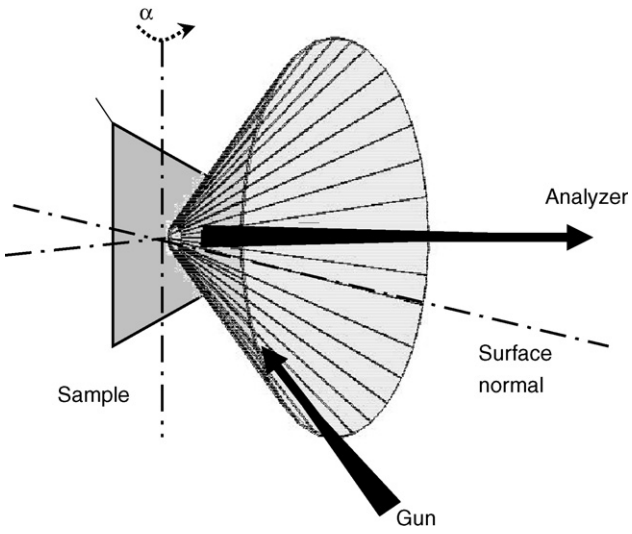

Fig. 1. A sketch of the experimental setup employed in this paper. The sample surface normal is horizontal. The electron gun is in the vertical plane through this surface normal, the detector is in the horizontal plane through this surface normal. Both incoming and outgoing electrons make an angle of 45° with the surface normal.

In the case of elastic scattering experiments the electron gun emits a 500 eV electron beam. The analyzers operate at a pass energy of 200 eV, and the analyzers are floating at −300 V in order to measure the elastic peak. The sample and its surroundings are at a potential of 39.5 kV. Hence electrons are scattered from the sample with an energy of 40 keV. In order to assure that the elastic peak can be measured with good resolution the drift and ripple of the −300 (analyzer) and −500 V (filament) power supply should have a combined ripple and drift of less than 100 meV. Drift and ripple of the 39.5 kV power supply can be much larger than this value, without affecting the outcome of the measurement.

The opening angle of the analyzer is 1×10^{-4} sr. The analyzer is equipped with a two-dimensional detector, allowing an energy window of 30 eV to be measured simultaneously. Simultaneous detection of a range of energies is essential in order to complete these measurements in a manageable time, in spite of the small opening angles and the small large-angle elastic cross sections.

The beam current used varied from less than 1 nA for measurements of Pt films, to about 10 nA for the measurement of carbon films. The spectra were obtained in $\simeq$2 h, so the total charge accumulated by the sample was 2–5 μC for the Pt case and 70–90 μC for the HOPG samples. The beam spot size was 0.1 mm^2.

The sample can be rotated around the vertical axis, and this angle is called α. In this experiment $\alpha = 0^\circ$ and the sur-

face normal of the sample is along the axis of the cone (and $\theta_{in} = \theta_{out} = 45^\circ$). Aluminum was evaporated from a boron-nitride crucible, and the thickness of the evaporated films were determined from the reading of the crystal thickness monitor. The crystal thickness monitor was calibrated using (ion) RBS.

3. Results and discussion

We inserted a freshly cleaved highly oriented pyrolytic graphite (HOPG) sample and a platinum foil into the vacuum chamber. The HOPG sample was measured as is, and the Pt sample after sputter-cleaning using 3 keV Xe^+ ions. These spectra are shown in the top of Fig. 2. Spectra shown in this figure are normalized to the same integrated charge (beam current × measurement time). This charge measurement was only approximate, as the contribution of secondaries and reflected electrons to the measured beam was not corrected for. The maximum intensity of the Pt spectrum (60,000 counts) is, however, 750 times the normalized maximum intensity of the HOPG sample (80 counts). This large difference can be understood from the large difference in cross section (see Table 1) in combination to the much larger width of the HOPG elastic peak. For scattering from carbon atoms, the Doppler broadening is large, chiefly due to the small mass of the carbon atoms (see Eq. (1)), and determines completely the width of the C elastic peak [9]. The width of the Pt peak, with its large mass will be mostly determined by the experimental energy resolution.

The zero point of the energy scale is only known approximately. It was adjusted in such a way that the elastic peak is not at zero energy loss, but at $\overline{E_r}(M)$ (5.7 eV for the HOPG film and 0.36 eV for the Pt film). Besides the main elastic peak the spectra show the familiar energy loss features at an additional 6 and 25 eV energy loss for HOPG corresponding to the π and the $\sigma + \pi$ plasmon [10]. For Pt several less pronounced additional loss structures are seen at positions in agreement with the energy of volume electronic excitations as reported in the literature [11].

After Al deposition a new peak is observed near the original elastic peak. This peak appears at the same energy loss value for both the Pt and HOPG substrate. It is at, or very close to, an energy loss value of 2.52 eV, i.e. the $\overline{E_r}(M)$ value of Al, and is thus attributed to electrons scattering elastically from Al. This validates the energy-zero alignment procedure followed. The Al

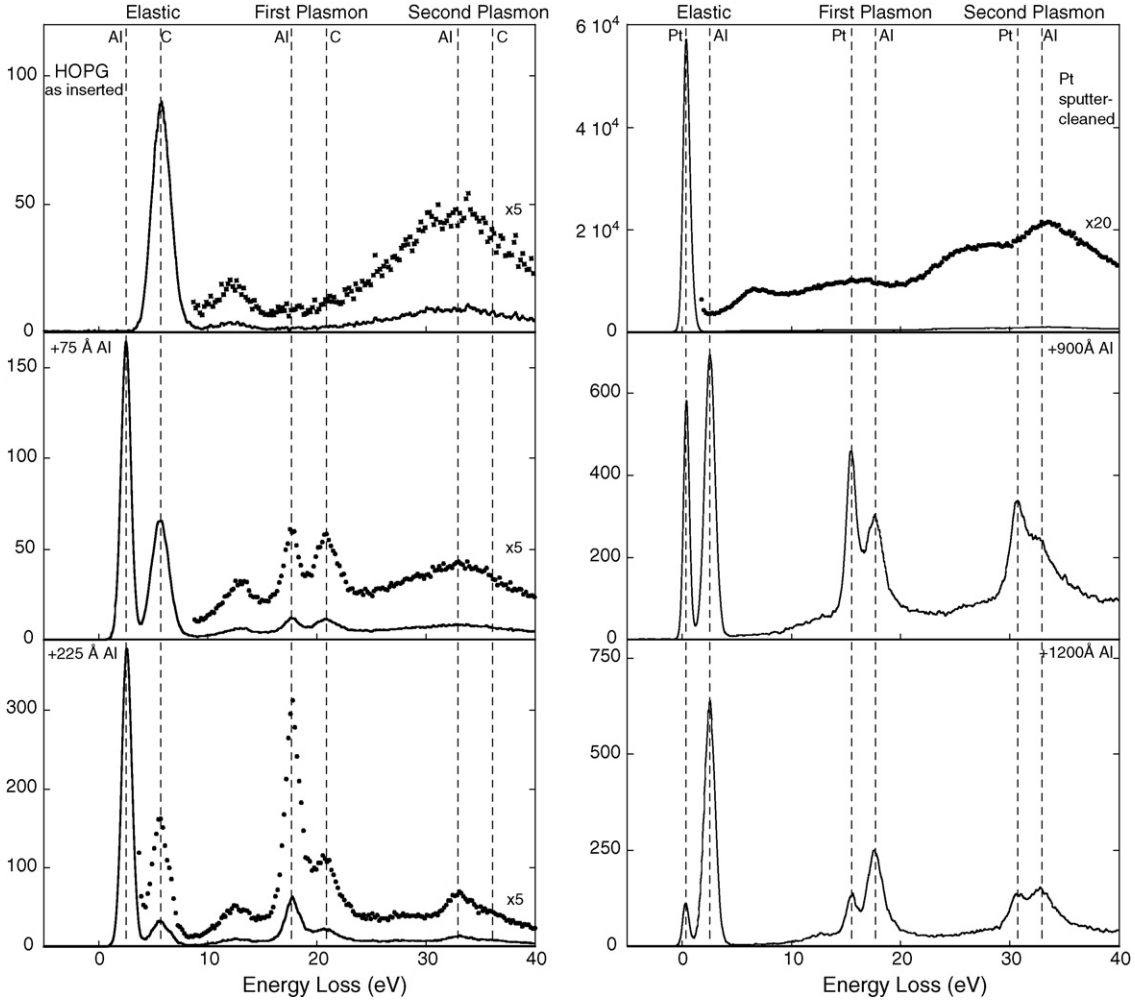

Fig. 2. Comparison of measured REELS spectra of HOPG and Pt before and after Al deposition. The dashed lines marked elastic peak are separated by the difference in the recoil energy of Al and C and Al and Pt, respectively. The dashed lines marked first and second plasmon are separated by 15.2 eV and 2 × 15.2 eV from the respective elastic lines.

Table 1
Various calculated and observed quantities pertaining to elastic scattering for different elements

Elements	$\overline{E_r}$ (eV)	$\Delta\overline{E_r}$ (Al) (calculated; eV)	$\Delta\overline{E_r}$ (Al) (observed; eV)	Width (FWHM; eV)	$d\sigma/d\Omega$ (cm^2)	λ_{in} (Å)
C	5.70	3.17	3.08	2.0	5.0×10^{-23}	405
O	4.27	1.74	–	1.6	9.0×10^{-23}	–
Al	2.53	0	0	1.1	2.44×10^{-22}	528
Xe	0.52	−2.01	−2.01	0.84	6.33×10^{-21}	–
Pt	0.36	−2.17	−2.13	0.66	1.70×10^{-20}	237

The calculated mean recoil energy $\overline{E_r}$ cannot be directly compared to the experiment, as the zero energy loss position of the spectra is only approximately known. The calculated difference between the recoil energy of various elements with the recoil energy of Al can be compared to the experiment. The observed width of the elastic peak is determined by both experimental resolution and Doppler broadening. The differential elastic scattering cross section $d\sigma/d\Omega$ at 120°, 40 keV was obtained from the ELSEPA package [12], the inelastic mean free path was obtained from the TPP-2M formula [13] except in the case of graphite, where we used the value obtained from Ref. [14].

peak appears at the high-energy loss side of the main peak in the case of the Pt film, and at the low-energy loss side for the HOPG film. Its width is larger than the width of the Pt peak but smaller than the width of C peak, consistent with decreasing Doppler broadening with increasing atom mass.

Besides the additional elastic peak two new peaks appear at larger energy loss values. We interpret *both* peaks to be due to Al plasmon excitations. The splitting of the two plasmon peaks is the same as the splitting of the elastic peaks. Thus, the interpretation for the cause of the splitting of the plasmon peak is straight-forward. The plasmon creation itself causes only a minor deflection of the energetic electron ($\ll 1°$) and a large-angle elastic scattering event from either a heavy or a light atom is required for the electron to be detected. The recoil energy loss of this scattering adds to the energy loss of the plasmon excitation. The plasmon peak appears thus not at 15.2 eV but at $15.2 + 0.4$ eV (elastic scattering from Pt), $15.2 + 2.5$ eV (elastic scattering from Al) and $15.2 + 5.7$ eV (elastic scattering from C). We refer to these peaks in the rest of this paper as the Pt plasmon peak, Al plasmon peak and C plasmon peak, respectively. In all cases the plasmon refers to the collective excitation in the Al film, and Pt, Al and C refers to the atom from which the electron scattered elastically over a large angle.

In Fig. 2 we show the spectra obtained for films where both plasmon components have similar intensities. Note that this occurs at rather different overlayer thicknesses for the HOPG and the Pt substrate. This is a consequence of the different elastic scattering cross section of both elements.

After Al deposition we also see a strong second plasmon for the Pt substrate. Even the second plasmon is clearly composed of two components, although the splitting is less resolved presumably due to the larger intrinsic width of the second plasmon peak ($\simeq \sqrt{2}$ times larger than the width of a single plasmon excitation). For the Al depositions on a HOPG substrate, the intensity of the second plasmon is less than the statistical uncertainty. This small intensity is no surprise as the Al film thickness is less than the inelastic mean free path, and hence the chance of two plasmon excitations occurring in this film is small.

It is clear from inspecting Fig. 2 that the intensity distribution of the two plasmon-derived peaks is not proportional to the intensity distribution of the two elastic peaks. For example, for the 75 Å Al-on-HOPG case the plasmon-derived peaks have about the same intensity, whereas the elastic Al peak is much stronger than the elastic C peak. For the 1200 Å Al-on-Pt case the intensity of the two components differs by an order of magnitude for the elastic peak, but only by about a factor of two for the single plasmon-loss peak. In this case even the second plasmon is clearly split, and for this peak the intensity is fairly evenly distributed over both components. We will argue that with larger energy loss the spectrum reflects the composition of the sample at increasing depth. This requires a more quantitative description of the experiment and we use curve fitting to decompose the elastic peak and the plasmon loss peak in the two components.

In order to restrict the number of free fitting parameters we first studied a pure Al film. Unfortunately, as is obvious from Fig. 3, the Al elastic peak shows a shoulder at larger energy loss. This shoulder appears consistent with the presence of oxygen at the surface that is within the detection limit, even at these, rather high, electron energies. A peak decomposition assuming that the separation is that calculated for oxygen was done. The area of the oxygen-related elastic peak is $\simeq$6.5 times smaller than the main peak (see insert Fig. 3). Assuming that this peak is due to oxygen atoms in an Al_2O_3 layer, and cross sections as in Table 1, then about 1/3 of the Al peak would be due to Al^{3+} ions in the oxide layer. Prolonged sputtering with Xe^+ ions at 3 keV removes the shoulder (lower panel Fig. 3). However, now a new feature appears at the high-energy loss side. We attribute this to implanted Xe^+ ions, and indeed the observed peak separation is that expected for Al–Xe (see Table 1).

The plasmon peak of the as-inserted sample could not be fitted very well with a single Gaussian and a linear background. The peak appears broader at the high-energy loss side. This is presumably a consequence of the dispersion of the plasmon, as we sample plasmons with different momentum values equally well, as explained in Section 1. The slower decay at larger energy loss will thus be due to plasmons with larger momentum and hence energy. Empirically we fit the plasmon with two Gaussian components, separated by 1 eV. The main component had a full width at half maximum (FWHM) of 1.45 eV. The second component at higher energy loss values is broader (FWHM 4.6 eV) and less intense (area 0.45 of the area of the main peak) (see Fig. 4). After sputtering a new shoulder appears in the loss structure at the low-energy loss side. We interpret this to be due to electrons that were scattered elastically from Xe instead of Al. We decomposed this feature assuming the structure could be described by two pairs of Gaussians. One pair due to electrons

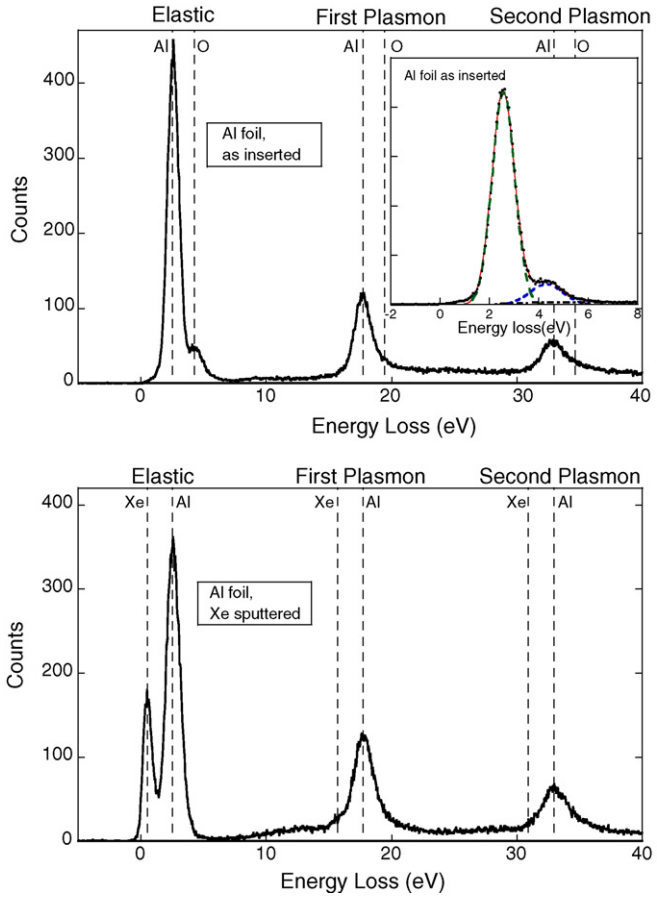

Fig. 3. Spectra from an Al foil before and after sputtering with 3 keV Xe^+ ions. Before sputtering the elastic peak has a shoulder at the high-energy loss side. The insert shows decomposition of this elastic peak in two components, using the separation calculated for oxygen and Al. After sputtering a strong contribution due to implanted Xe^+ ions appear at the low-energy loss side of the Al peak.

scattered elastically from Xe and one pair for electrons scattered from Al. The two Gaussians in each component have the same intensity ratio and 1 eV separation as the two Gaussians in the 'as inserted' Al plasmon fit. The displacement of the two components was taken from the separation of the components of the elastic peak. The width was considered to be the convolution of the plasmon loss width and the width of the elastic peak due to Doppler broadening. Thus, the plasmon loss feature of the Xe-related component was somewhat sharper than the plasmon loss feature of Al-related component. In this way we can fit the two peak structures, while having only 4 fitting parameters (intensity of the main component, intensity of the second component, and two parameters for the linear background).

The same procedure outlined for the sputtered sample was followed for the Al-HOPG and Al-Pt data. All fits are shown in Fig. 4. The procedure seems to work reasonably well. However, different fitting procedures could be developed that give qualitatively somewhat different results. For example the assumption that the intensity under the plasmon can be described by a linear background is questionable. We do not expect, however, that the main trends, as will be discuss in the next section, would be very different. We also fitted the main elastic peak, using a single Gaussian for each component and a Shirley background. These fits were completely unambiguous. In this way we obtain the various intensity ratios reproduced in Table 2. We will now discuss these ratios.

The first column of results shows us the ratio of the areas of the elastic peaks $I_{el}^{Al} : I_{el}^{X}$. After sputtering the Xe peak area is significant, however the cross section of Xe is $\simeq 26$ times the cross section of Al. A Xe concentration of a few % in the near surface area would result in such a peak. For the HOPG sample a modest Al layer of 75 Å results in two elastic peaks of comparable size. Tripling the Al thickness changes the elastic peak ratio by more than a factor of 5. As the plots in Fig. 2 are normalized to the same integrated charge we can see the cause of this large change. The Al intensity more than doubles, as the layer gets three times as thick, and the HOPG intensity is attenuated by close to a factor of 2.

The situation is different for the Pt substrate. Now we need a very thick (900 Å) Al layer in order to get the elastic peaks of the same order of magnitude. Increasing the Al layer from 900 to 1200 Å changes the ratio by more than a factor of 4. Now however, this change is almost exclusively due to increased attenuation of the Pt signal. The Al intensity is virtual constant, as it is is already very close to the Al intensity of an infinitely thick Al layer.

If one makes a number of simplifying assumptions (homogenous Al layer thickness, abrupt substrate/overlayer interface, and a single elastic scattering approximation for the electron trajectories) then it is fairly straight forward to calculate intensity ratio for the elastic peaks based on the material properties reproduced in Table 1. This procedure was described in Ref. [4]. For the 900 Å thick Pt layer we obtain a Al to Pt peak ratio of 1:0.28 (observed 1:0.48) and for the 1200 Å layer 1:0.055 (observed 1:0.11). Clearly the agreement between calculated values and observed values is poor. This can be seen as an indication that one of the fore-mentioned assumptions is not valid. In the Al-

Table 2
The ratio of the intensity of the elastic peaks, the intensity ratio of the Al elastic peak to the Al plasmon peak and this ratio for the second component (X) as well as the ratio of the plasmon peaks

Sample	X	$a = I_{el}^{Al} : I_{el}^{X}$	$I_{el}^{Al} : I_{pl}^{Al}$	$I_{el}^{X} : I_{pl}^{X}$	$b = I_{pl}^{Al} : I_{pl}^{X}$	$a : b$
Xe sputtered Al	Xe	1:0.32	1:0.52	1:0.10	1:0.06	$0.06/0.32 = 0.19$
75 Å on HOPG	C	1:0.71	1:0.08	1:0.14	1:1.2	$1.2/0.71 = 1.7$
225 Å on HOPG	C	1:0.13	1:0.24	1:0.59	1:0.33	$0.33/0.13 = 2.5$
900 Å on Pt	Pt	1:0.48	1:0.59	1:1.53	1:1.24	$1.24/0.48 = 2.6$
1200 Å on Pt	Pt	1:0.11	1:0.59	1:1.81	1:0.33	$0.33/0.11 = 3.0$

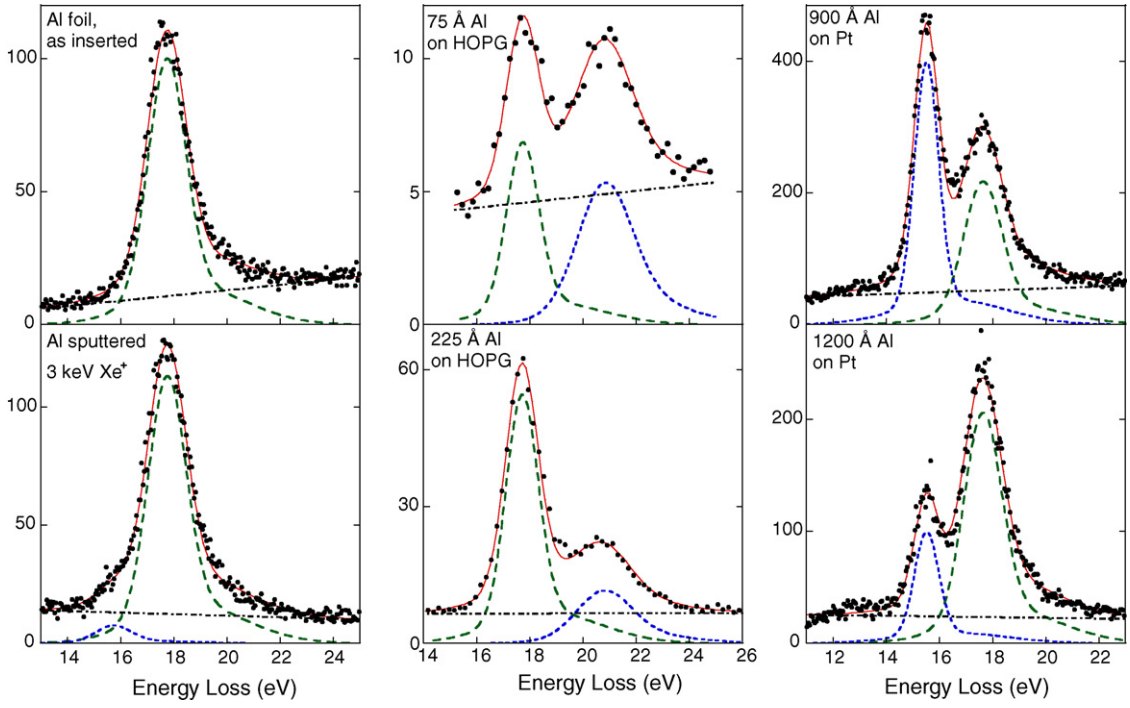

Fig. 4. Overview of the fits of the Al plasmon peak for pure Al before and after sputtering (left column), as well as for Al deposited on HOPG (centre) and Pt (right). The fitting procedure is explained in the main text.

on-Pt case the calculated ratios are most sensitive to the assumed inelastic mean free path. Thus, deviations of the inelastic mean free path from the TPP-2M values could be the cause of the discepancy. One can obtain a 'perfect' fit of the experimental data by changing the Al inelastic mean free path from 528 Å to 590 Å and the Pt inelastic mean free path from 237 Å to 270 Å. However, spectra taken at lower Al coverage seem to indicate that the assumption that the Pt-Al interface is abrupt is not valid, and this will, at least in part, be the cause in the difference of the observed and calculated elastic peak ratio for the Pt case.

Next consider the intensity ratio of the Al elastic peak to the Al plasmon peak: $I_{\mathrm{el}}^{\mathrm{Al}} : I_{\mathrm{pl}}^{\mathrm{Al}}$. For very thin layers the path length of the trajectories within the Al layer is very short, hence the chance that a plasmon is created is very small. Increasing the film thickness will increase the path length of electrons scattered elastically from an Al atom in the Al film, and hence the relative intensity of the plasmon peak relative to the Al elastic peak will increase for very thin films linearly with thickness. On the other hand if we make the layer very thick, then the relative plasmon intensity will approach the value for a bulk film, and will not change anymore with thickness. From the observed ratios it is clear that the 75 Å and 225 Å thick Al films are still in the regime that the plasmon intensity increases almost linearly with thickness. For the 900 Å and 1200 Å measurement the intensity ratio seems to be independent of thickness, i.e. we are in the bulk limit. The value after Xe^+ bombardment is somewhat smaller than for the 900 Å and 1200 Å thick films. It is not clear why this is the case, and could be an indication of the limits of the validity of the very simple fitting procedure followed.

The ratio of the (C, Pt, Xe) elastic peak to the (C, Pt, Xe) plasmon ($I_{\mathrm{el}}^{\mathrm{X}} : I_{\mathrm{pl}}^{\mathrm{X}}$) should be determined by the length of the trajectories through the Al film of events scattering from these atoms. This length is shortest for Xe as the mean range of 3 keV Xe^+ ions in Al (impinging at 45°) is close to 40 Å [15]. For the evaporated layers the relative intensity of $I_{\mathrm{pl}}^{\mathrm{X}}$ increases roughly linearly with Al thickness.

In transmission electron microscopy work one can measure,using a small opening aperture (at zero degrees scattering angle), spectra for which only plasmons with zero momentum contribute. In that case there is very little intensity besides the plasmon peak in the loss spectrum. Then the probability that an electron is detected after being transmitted through a film of length τ while exciting n plasmons is given by a Poisson distribution [6]:

$$I_n = \left(\frac{1}{n!}\right)\left(\frac{\tau}{\lambda_0}\right)^n \exp\left(\frac{-\tau}{\lambda_0}\right). \tag{2}$$

The ratio of the intensity of the elastic peak ($n = 0$) and the first plasmon peak is then simply, $1 : \tau/\lambda_0$. From the point of view of electrons scattered elastically from the substrate this experiment resembles a transmission experiment, both the incoming and scattered electrons are transmitted through the Al layer. Thus, in this case $\tau = 2t/\sin 45^\circ$ with t the thickness of the film. Here λ_0 is the mean free path for the creation of plasmons detected by the microscope (i.e. those excitation that cause very limited deflection). It is about twice as large as the mean free path for all electronic excitations [5]. In our case we detect in first approximation all electrons equally well, independent from the degree of deflection by the inelastic scattering event. This is obvious from the energy loss spectrum of Al, where about half the intensity of electrons with energy loss is not related to the plasmon peaks. These events are better described by electron-electron collisions,

rather than collective excitations. Thus, translation of the electron microscopy model to the present case is not totally straight forward. If we apply the electron microscopy model, in spite of these reservations, then we get for the ratio for the Pt experiment a value of $\lambda_0 \simeq 1700$ Å. This value is 3–4 times λ of aluminum (see Table 1), clearly this value is too large.

Next consider the column in Table 2: the ratio of the plasmon intensities $I_{\mathrm{pl}}^{\mathrm{Al}} : I_{\mathrm{pl}}^{\mathrm{X}}$. The ratio is smallest for Xe. This is an indication that the Xe ions are close to the surface. The length of the trajectory of electrons scattering from Xe in Al is small, hence the probability that an electron scattering from Xe creates a plasmon is small. For both Pt and HOPG the relative intensity of the Al plasmon to the Pt increases with overlayer thickness.

These ratios are determined by the elastic scattering cross section of the overlayer and substrate hence we cannot compare the ratios of the Pt experiment and the HOPG experiment However, the ratio of the elastic peaks is affected in the same way by these cross sections. Dividing $a = I_{\mathrm{el}}^{\mathrm{Al}} : I_{\mathrm{el}}^{\mathrm{X}}$ by $b = I_{\mathrm{pl}}^{\mathrm{Al}} : I_{\mathrm{pl}}^{\mathrm{X}}$ the cross section effect will cancel. This ratio $a : b$ is shown in the last column of Table 2. For the overlayer experiment we get now numbers larger than 1. This means that in the plasmon signal from the substrate is relatively larger than from the elastic peak, i.e. it is more bulk sensitive. This ratio increases gradually with overlayer thickness.

For the Xe case the Xe signal originates from a depth much smaller than the inelastic mean free path. Hence here this ratio is thus smaller than 1. The more-bulk sensitive plasmon signal shows relatively less intensity of the Xe near-surface impurity. Of course the signal from impurities right at the surface there should not have a corresponding Al plasmon peak, and the ratio $a : b$ would be 0.

4. Discussion and conclusion

From Fig. 2 it is clear that the Al peak dominates the C peak after 225 Å Al deposition, whereas for the Pt case this happens near 1200 Å. This is a consequence of the much stronger signal obtained from Pt compared to the signal of C, i.e. due to the different elastic scattering cross sections. Thus, the probing depth in this technique is larger for the Pt/Al experiment than the C/Al experiment. Generally the probing depth for overlayer substrate systems is large for a low-Z overlayer on a high-Z substrate, and small for the reversed situation. This was predicted based on Monte Carlo simulations [16,17] and confirmed experimentally for the Au–C system [4]. Here we see another consequence of the large probing depth for the Pt substrate. The large area of the plasmon corresponding to elastic scattering from Pt, compared to the Pt elastic peak itself is a sign of the long trajectories inside the Al layer for these scattering events.

In the HOPG case the Al plasmon was well developed after 75 Å Al deposition. This means that the interface is reasonable abrupt, and compound formation at the interface is limited to layers smaller than 75 Å. For the Pt case the Al plasmon is not well developed after 75 Å Al deposition, indicating a more diffuse interface. Thus, monitoring the elastic peak height of mass-resolved elastic peaks in combination with the shape of the REELS spectrum can provide useful information. The methods described here could provide a unique opportunity to study rather thick layers by electron spectroscopy, formed either by evaporating on a reactive surface, or by annealing overlayers of more inert systems, that form compounds. Currently we are studying the interface formation of these more reactive interfaces by this technique.

Depth information, as obtained here, could also be obtained by tilting the sample as this is known to affect the observed elastic peak signals strongly [4]. If one would utilize this method in an electron microscope, using a well focussed beam, then tilting the sample would almost inevitably change the position where the beam impinges on the sample, and spatially-resolved depth resolution would be hard to obtain. The method described here does not have this drawback. An interesting case would be Xe implanted Al, where the Xe is known to form bubbles (see, e.g. [18]). By aligning the focussed beam with a single Xe bubble the intensity of the Xe derived plasmon would provide a measure of the depth of a particular Xe bubble.

In summary we have shown that differences in recoil energies (depending on the mass of the scatterer) in elastic scattering can still be resolved if a plasmon with well-defined energy is excited by the incoming or outgoing electrons. The relative intensity of the different plasmon components provides us with information about the depth distribution of the scatterer. The combination of the elastic peak intensities and plasmon peak intensities (and the energy loss distribution in general) opens up unique opportunities to study relatively thick overlayers by electron spectroscopy.

Acknowledgements

We are grateful for the ion RBS measurement by Rob Elliman used to calibrate the crystal thickness monitor. This work was made possible by a grant of the Australian Research Council.

References

[1] M.R. Went, M. Vos, Surf. Sci. 600 (10) (2006) 2070–2078.
[2] M. Went, M. Vos, Appl. Phys. Lett. 90 (2007) 072104.
[3] M. Went, M. Vos, R.G. Elliman, J. Electron Spectrosc. Relat. Phenom. 156–158 (2007) 387.
[4] M. Vos, M.R. Went, Surf. Sci. 601 (2007) 1536.
[5] P.E. Batson, J. Silcox, Phys. Rev. B 27 (9) (1983) 5224–5239.
[6] R.F. Egerton, Electron Energy-loss Spectroscopy in the Electron Microscope, second ed., Plenum Press, New York, 1996.
[7] W.S.M. Werner, Surf. Interface Anal. 31 (2001) 141–176.
[8] M. Vos, G.P. Cornish, E. Weigold, Rev. Sci. Intrum. 71 (2000) 3831–3840.
[9] M. Vos, M.R. Went, Phys. Rev. B 74 (2006) 205407.
[10] H. Raether, Excitation of Plasmons and Interband Transitions by Electrons, Springer Tracts in Modern Physics, vol. 88, Springer Verlag, Berlin, 1979.
[11] W.S. Werner, Surf. Sci. 588 (2005) 26.
[12] F. Salvat, A. Jablonski, C.J. Powell, Comput. Phys. Commun. 165 (2005) 157–190.
[13] S. Tanuma, C.J. Powell, D.R. Penn, Surf. Interface Anal. 20 (1993) 77.
[14] S. Tanuma, C.J. Powell, D.R. Penn, Surf. Interface Anal. 37 (2005) 1–14.
[15] J. Ziegler, J. Biersack, U. Littmark, The Stopping and Range of Ions in Solids, Pergamon Press, New York, 1985.
[16] L. Zommer, A. Jablonski, J. Electron Spectrosc. Relat. Phenom. 150 (2006) 56–61.
[17] L. Zommer, Surf. Sci. 600 (2006) 4735.
[18] A. vom Felde, J. Fink, T. Müller-Heinzerling, J. Pflüger, B. Scheerer, G. Linker, D. Kaletta, Phys. Rev. Lett. 53 (9) (1984) 922–925.